International Journal of Applied Pharmaceutics

ISSN- 0975-7058 Vol 11, Issue 6, 2019

Original Article

FORMULATION AND CHARACTERIZATION OF TIMOLOL MALEATE-LOADED NANOPARTICLES GEL BY IONIC GELATION METHOD USING CHITOSAN AND SODIUM ALGINATE

RISA AHDYANI[1,2], LARAS NOVITASARI[1], RONNY MARTIEN[1*], RETNO DANARTI[3]

[1]Departement of Pharmaceutics, Faculty of Pharmacy, Universitas Gadjah Mada, Sekip Utara, D. I. Yogyakarta 55281, Indonesia, [2]Department of Pharmaceutics, Faculty of Pharmacy, Universitas Muhammadiyah Banjarmasin, Kalimantan Selatan, 70114, Indonesia, [3]Department of Dermatology and Venereology, Faculty of Medicine, Public Health and Nursing, Universitas Gadjah Mada, Farmako Sekip Utara, D. I. Yogyakarta 55281, Indonesia
Email: ronnymartien@ugm.ac.id

Received: 18 Jul 2019, Revised and Accepted: 02 Sep 2019

ABSTRACT

Objective: The objectives of this study were to formulate and characterize nanoparticles gel of timolol maleate (TM) by ionic gelation method using chitosan (CS) and sodium alginate (SA).

Methods: Optimization was carried out by factorial design using *Design Expert*®10.0.1 software to obtain the concentration of CS, SA, and calcium chloride ($CaCl_2$) to produce the optimum formula of TM nanoparticles. The optimum formula was characterized for particle size, polydispersity index, entrapment efficiency, Zeta potential, and molecular structure. Hydroxy Propyl Methyl Cellulose (HPMC) K15 was incorporated into optimum formula to form nanoparticles gel of TM and carried out *in vivo* release study using the Franz Diffusion Cell.

Results: TM nanoparticles was successfully prepared with concentration of CS, SA, and $CaCl_2$ of 0.01 % (w/v), 0.1 % (w/v), and 0.25 % (w/v), respectively. The particle size, polydispersity index, entrapment efficiency, and Zeta potential were found to be 200.47±4.20 nm, 0.27±0.0154, 35.23±4.55 %, and-5.68±1.80 mV, respectively. The result of FTIR spectra indicated TM-loaded in the nanoparticles system. *In vitro* release profile of TM-loaded nanoparticles gel showed controlled release and the Korsmeyer-Peppas model was found to be the best fit for drug release kinetics.

Conclusion: TM-loaded CS/SA nanoparticles gel was successfully prepared and could be considered as a promising candidate for controlled TM delivery of infantile hemangioma treatment.

Keywords: Timolol maleate, Nanoparticles, Infantile hemangioma

DOI: http://dx.doi.org/10.22159/ijap.2019v11i6.34983

INTRODUCTION

Infantile hemangioma (IH) is the most prevalent vascular benign tumor in children with an incidence of about 4 to 10 % in the first year of life [1]. Although it will improve spontaneously, about 10 to 20 % of infants who have IH require interventions to prevent and reduce complications associated with the proliferation phase [2]. In addition, IH has implications for parental psychology and visual disfigurement of children [3]. IH can occur in any part of the body, but the most often found in the head and neck area so that it can trigger deformity [4]. Topical TM is a promising alternative treatment for IH. The use of topical TM for IH treatment was first reported in 2010. Since then, many case reports and case series have demonstrated the efficacy of TM for the treatment of IH. TM can inhibit growth and promote the regression of IH [5]. However, TM has systemic absorption due to it is administered topically and then result in unwanted effects [6].

The therapeutic effectiveness of topical dermatology formulation can be improved by nanotechnology-based delivery systems. Nanoparticles are of great interest in drug delivery due to their comparable size of the component in the human cell. Size matching is important in carrying out any activities in the biological system [7]. The successful implementation of nanoparticles for drug delivery depends on their ability to penetrate through several anatomical barriers, sustained release of their contents, and their stability in the nanometer size [8]. Polymeric nanoparticles are solid colloidal particles with a diameter ranging from 1 nm to 1000 nm. It is developed by using biodegradable and biocompatible polymers offer interesting options for controlled drug delivery and drug targeting [9].

Biopolymers are polymer molecules that have been used extensively as biomaterials in drug delivery systems. The use of biopolymers has several advantages due to their properties, such as biocompatible, non-toxic, non-irritant, and can form the network of particles matrix. The preparation of biopolymers system uses double polymer which has opposite charges to form a matrix, so it can trap drug molecules. CS and SA are great combinations of biopolymers that can be used in drug delivery system [10]. Biopolymeric nanoparticles of CS and SA can deliver active ingredients with controlled drug release profile. Therefore, it can increase the efficacy of therapy, reduce systemic drug absorption, and reduce the frequency of administration [11].

CS/SA nanoparticles can be prepared by ionic gelation methods using ions of calcium. Mechanism of interaction is based on the negative charge of the uronic acid carboxylic groups of SA with the positive surface charge of the protonated amino groups of CS. The formation of CS/SA nanoparticles by the ionic gelation method produces a pre-gel that consists of very small aggregates of gel particles, which are then followed by the addition of a polycationic solution to form the polyelectrolyte complex. CS/SA nanoparticles can protect drug encapsulation from enzymatic degradation, drug delivery to target organs, prolong contact time of active ingredients with target epithelial cells, and control drug release [12].

MATERIALS AND METHODS

Materials

TM was purchased from Octagon Chemical Limited (China), CS (molecular weight: 200 kDa to 500 kDa with 94.88 % of deacetylation degree) was purchased from local company Chimultiguna (Cirebon, Indonesia), SA was purchased from Sigma Aldrich (Darmstadt, Germany), $CaCl_2$ was purchased from Merck (Germany), glacial acetic acid, hydrochloric acid, and sodium hydroxide were purchased from Merck (New Jersey, USA).

Optimization of TM nanoparticles

Optimization of TM nanoparticles was prepared based on the 2^3 factorial design to select independent variables that were needed to

produce the optimum formula of TM nanoparticles. The selected three independent variables were the concentration percentage of CS, SA, and $CaCl_2$.

Characterization of TM nanoparticles

Particle size, polydispersity index, and Zeta potential

Particle size, polydispersity index, and Zeta potential were analysed by the method of dynamic light scattering (DLS). The TM nanoparticles was examined using Zetasizer Nano ZS (Malvern, UK) to determine the average of particle size and polydispersity index (distribution of particles). A certain amount of TM nanoparticles sample was dispersed in 5 ml of aquadest and then placed in disposable cuvette. Zeta potential of TM nanoparticles was also examined using Zetasizer Nano ZS (Malvern, UK) to determine surface charge of particles. A certain amount of TM nanoparticles was placed in dip cell carefully. Replications were done for each measurement of the same samples for 3 times. This instrument was controlled with Malvern software [13].

Entrapment efficiency

Entrapment efficiency (EE) of TM nanoparticles was measured inderectly. Samples of TM nanoparticles were sentrifugated using Refrigerated Centrifuge (Velocity 18R) at 15 000 rpm for 30 min at 4 °C to separate unloaded nanoparticles. The clear supernatant (unloaded nanoparticles) was analyzed using UV-Vis spectro-photometer (Thermo Scientific Genesys 10S UV) at 296 nm. The following equation was used to calculate entrapment efficiency (EE) [12].

$$EE\ (\%) = \frac{\text{total amount of TM} - \text{unloaded nanoparticle of TM in supernatant}}{\text{total amount of TM}} \times 100$$

Structure characterization

Structure characterization of optimum formula of TM nanoparticles was analysed using Fourrier Transform Infra-Red (FTIR) spectrophotometer (Thermo Scientific Nicolet iS10, Madison, WI). This instrument was controlled with Omnic software. The measurements were done in middle infrared region of 4000-650 cm^{-1}. Replications were done for 3 times [13].

Preparation of TM-loaded nanoparticles gel

HPMC K15 was incorporated into optimum formula aqueous, and then stirred to form homogenous gel of TM nanoparticles. Furthermore, the physicochemical properties of nanoparticle gel of TM were evaluated.

***In vivo* release study of TM-loaded nanoparticle gel**

In vivo release study of TM-loaded nanoparticle, gel was carried out using the Franz Diffusion Cell. This study was done through the dialysis membrane with a molecular weight cut-off 6 to 8 kDa. The phosphate buffer solution (pH = 5.8) was placed in receptor compartment. Next, 5 ml of nanoparticles gel loaded TM was placed in compartment donor on a dialysis membrane. The system of medium temperature was controlled at 37±0.5 °C and was stirred continuously using magnetic stirrer. Furthermore, at intervals times 1, 2, 3, 4, 5, 6, 7, 8, 12, 16, 20, and 24 h, amount of 3 ml of the medium was removed and the same quantity was replaced. TM released from nanoparticles was analyzed using UV-Vis spectrophotometer (Thermo Scientific Genesys 10S UV) at 297 nm [14].

Statistical analysis

Statistical analysis was carried out using *Design Expert*®10.0.1 software for optimum formula of TM nanoparticles and DDSolver program for release profile of TM-loaded CS/SA nanoparticles gel.

RESULT AND DISCUSSION

Particle size, polydispersity index, and entrapment efficiency

Table 1: The result of an average of particle size (nm), polydispersity index, and entrapment efficiency (%) as the response of full factorial design experimental (n=8)

Formulation codes	Independent variables			Responses		
	CS	SA	$CaCl_2$	Particle diameter (nm)	Polydispersity index	Entrapment efficiency (%)
F1	-1	-1	-1	473.10±75.86	0.37±0.0582	33.71±4.73
F2	+1	-1	-1	676.33±107.76	0.51±0.0489	33.20 ±7.16
F3	-1	+1	-1	489.30±15.14	0.51±0.0934	39.01±2.86
F4	+1	+1	-1	350.00±64.88	0.66±0.0345	37.59±3.86
F5	-1	-1	+1	200.47±4.20	0.27±0.0154	35.23±4.55
F6	+1	-1	+1	589.23±9.93	0.45±0.0326	33.71±3.99
F7	-1	+1	+1	447.83±100.54	0.49±0.0965	35.63±4.77
F8	+1	+1	+1	791.10±15.59	0.53±0.0349	39.77±3.01

*Data from each response is presented in mean±SD (n=3). CS (-1 = 0.01 % w/v; +1 = 0,1 % w/v), SA (-1 = 0.1 % w/v; +1 = 0.5 % w/v), $CaCl_2$ (-1 = 0.05 % w/v; +1 = 0.25 % w/v)

The particle size is a critical factor in the preparation of nanoparticles. The particle mean diameter obtained for all formulations were in range 200.47±4.20 nm to 791.10±15.59 nm (table 1). At the low concentration of CS (0.01 % w/v), SA (0.1 % w/v), and $CaCl_2$, (0.05 % w/v) particles diameter were obtained in range 200.47±4.20 nm to 489.30±15.14, 200.47±4.20 nm to 676.33±107.76 nm, and 350±64.88 nm to 676.33±107.76 nm, respectively. Meanwhile, at the high concentration of CS (0.1 % w/v), SA (0.5 % w/v), and $CaCl_2$, (0.25 % w/v) particles diameter were obtained in range 350±64.88 nm to 791. 10±15.59 nm, 350±64.88 nm to 791. 10±15.59 nm, and 200.47±4.20 nm to 791.10±15.59 nm, respectively. Based on the polynomial term of full factorial design experimental and contour plot that was showed in fig. 1 predicted effect of each independent variables to particle size. The greater concentration of CS, SA, and $CaCl_2$ was used in the formula; the greater particle size of nanoparticles was obtained. The main factor in nanoparticle formation is the tendency of functional groups of SA chains, especially carboxylic groups could form complex structures with calcium ions. These findings are in accordance with the previously study [15]. Daemi and co-worker reported that the high concentration of SA caused more functional groups to gather around calcium ions, then the more SA chains binded to form complexes with calcium cations.

Thus, the more concentration of SA used in the formula the larger size of particle produced. Meanwhile, increasing the concentration of calcium ions caused less amount of polymer chains involved with a greater content of calcium cations. So that, increasing of $CaCl_2$ led the smaller size of particle produced. Manish and co-workers were also reported that increasing the concentration of SA and CS increased particle size and ultimately decreased stability of nanoparticles due to aggregation and precipitation [16].

Polydispersity index describes the uniformity of particles size distribution produced. The smaller the polydispersity index obtained

the more uniform the particle size would be. Uniformity of the particle size distribution could affect the properties of particles produced due to it would not be easier to settle [17]. The polydispersity index value<0.5 indicates a narrow size distribution of particles. Meanwhile, polydispersity index value>0.5 indicates a broad particle size distribution of particles. Increase of polidispersity index could lead aggregation due to instable system [18].

The polydispersity index obtained for all formulations was in range 0.27±0.0154 to 0.66±0.0345 (table 1). At the low concentration of CS (0.01 % w/v), SA (0.1 % w/v), and $CaCl_2$ (0.05 % w/v) polydispersity index of nanoparticles were obtained in range 0.27±0.0154 to 0.51±0.0934, 0.27±0.0154 to 0.51±0.0489, and 0.37±0.0582 to 0.66±0.0345, respectively. Meanwhile, at the high concentration of CS (0.1 % w/v), SA (0.5 % w/v), and $CaCl_2$ (0.25 % w/v) polydispersity index of nanoparticles were obtained in range 0.45±0.0326 to 0.66±0.0345, 0.49±0.0965 to 0.66±0.0345, and 0.2±0.0154 to 0.53±0.0349, respectively. Based on polynomial term of full factorial design experimental and contour plot that was showed in fig. 2 predicted the effect of each independent variables to polydispersity index. The greater concentration of CS and SA were used in the formula the greater polydispersity index of nanoparticles was obtained. Meanwhile, the greater concentration of $CaCl_2$ the smaller polydispersity index was obtained.

Entrapment efficiency is an important parameter in the development of material based on the nanotechnology drug delivery system. The percentage of entrapment efficiency can provide an overview of the effectiveness of active binding compounds by polymer complexes in the nanoparticles system [19]. The percentage of entrapment efficiency obtained for all formulations was in range 33.20±7.16 % to 39.77±3.01 % (table 1). At the low concentration of CS (0.01 % w/v), SA (0.1 % w/v), and $CaCl_2$ (0.25 % w/v) percentage of entrapment efficiency of nanoparticles were obtained in range 33.71±4.73 % to 39.01±2.86 %, 33.20±7.16 % to 35.23±4.55 %, and 33.20±7.16 % to 39.01±2.86 %, respectively. Meanwhile, at the high concentration of CS (0.1 % w/v), SA (0.5 % w/v), and $CaCl_2$ (0.25 % w/v) percentage of entrapment efficiency of nanoparticles were obtained in range 33.20±7.16 % to 39.77±3.01 %, 35.63±4.77 % to 39.77±3.01 %, and 33.71±3.99 % to 39.77±3.01 %, respectively. Based on polynomial term of full factorial design experimental and contour plot that was showed in fig. 3 that predicted effect of each independent variables to percentage of entrapment efficiency. The greater concentration of CS, SA, and $CaCl_2$ was used in the formula the greater entrapment efficiency of nanoparticles was obtained. It is clear that increase in polymer concentration lead increases the drug entrapment efficiency [20].

The particle size, polydispersity index (PDI), and entrapment efficiency obtained through optimization of 8 formulas were used to generate the optimum formula of nanoparticles. Based on prediction of factorial design as a statictical tool, Formula 5 was selected as the optimum formula with concentration of CS, SA, and $CaCl_2$ 0.01 % (w/v), 0,1 % (w/v), and 0.25 % (w/v), respectively.

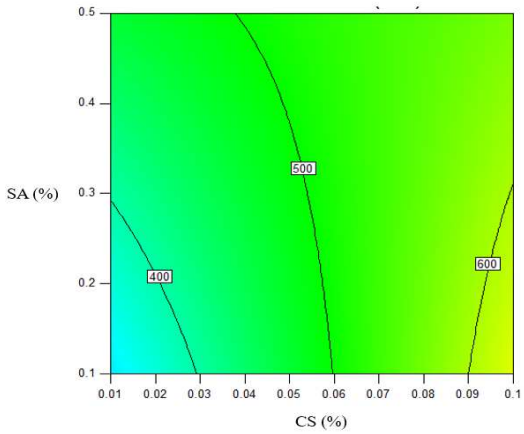

Fig. 1: The contour plot of particle size

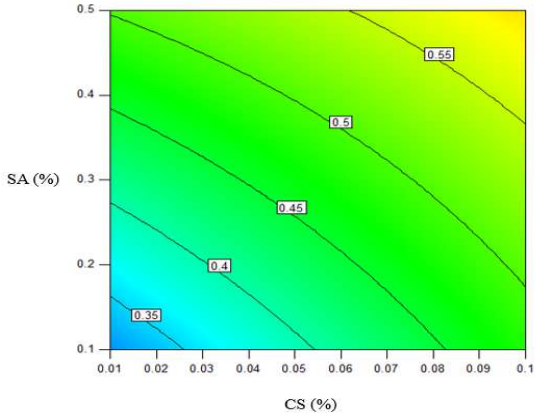

Fig. 2: The contour plot of PDI

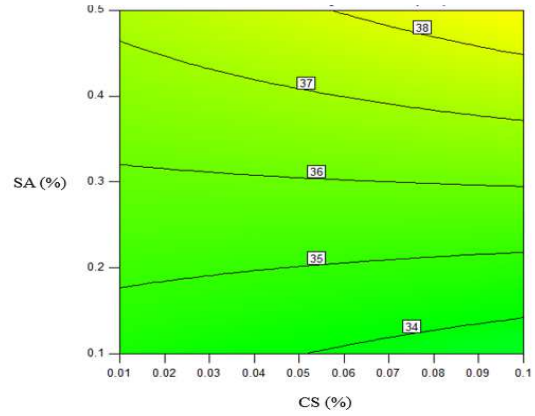

Fig. 3: The contour plot of entrapment efficiency

Zeta potential

Zeta potential describes the surface charge of particles. Zeta potential measurement is an important factor in determining the stability of the nanoparticles [21]. Zeta potential can describe the stability of nanosystem due to aggregation probability based on the Derjaguin, Landau, Verwey, dan Overbeek (DLVO) theory. The Van der Waals attraction and the electrostatic repulsion force are two forces that contribute to the stability of system. A high value of Zeta potential indicates a high repulsion force among particles due to electrostatic force, which is related proportionally to the Zeta potential of particles obtained. Thus, a high value of zeta potential can lead to a more stable of nanosystem [18]. Otherwise, a low value of Zeta potential may lead dispersion system to break and particle aggregation occurs. It is due to the attraction is greater than the repulsion force [20].

The Zeta potential that was produced by the optimum formula was found to be–5.68±1.80 mV and had a negative charge (fig. 4). This was related to the formation mechanism of nanoparticles through ionic gelation, due to the positive charge of the protonated NH_3^+groups of CS were neutralized through electrostatic interaction with the negative charge of polymeric SA and TM. The surface charge of particles was negative due to the electric potential of particles. It was influenced by the composition of the particles and the medium dispersed [20]. This result was accordance with the previously study [22]. The values of Zeta potential were highly influenced by the SA/CS ratio due to the Zeta potential of the SA/CS nano reservoir system was dependent on the availability of total protonated NH_3^+groups of CS and their neutralization with carboxylic groups of SA. When SA exceeded CS, the formulations showed negatively charged Zeta potential, which indicated carboxylic groups of SA were not sufficiently neutralized by the protonated NH_3^+ groups of CS. It was to be noted that the higher

percentages of SA revealed a negatively charged Zeta potential. Morsi and co-workers reported that the nanoparticles with small value of Zeta potential (-3.7 mV) despite having higher SA content and this probably because of the amounts of CS and $CaCl_2$ were still insufficient to interact with all carboxylic groups of SA. However, increasing the concentration of $CaCl_2$ or increasing the concentration of CS shifted the Zeta potential to positive values. These findings were also in accordance with the previously reported data [23]. Huang and co-workers reported that the negative value for Zeta potential of TM liquid crystalline nanoparticle.

FTIR analysis

The FTIR spectra could be used to get information about molecular structure from the vibration of functional groups at the certain wavenumber [24]. The FTIR spectra of TM nanoparticles were showed in fig. 5.

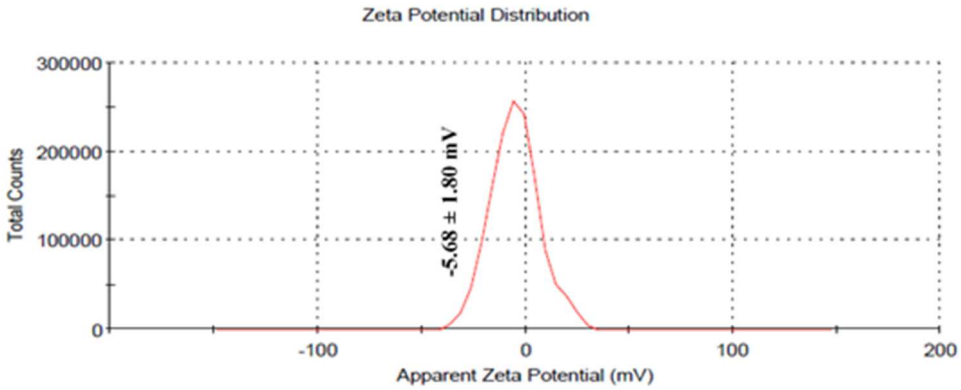

Fig. 4: Zeta potential distribution histogram showing–5.68±1.80 mV Zeta potential

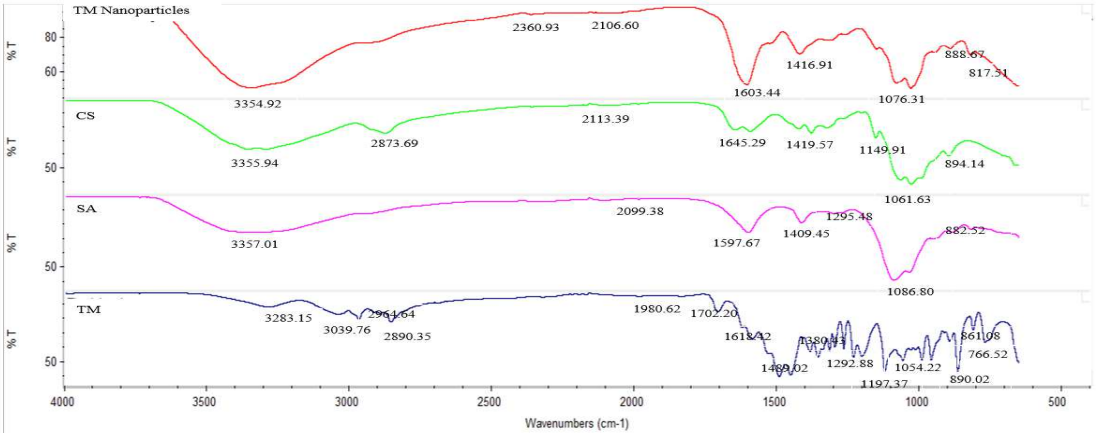

Fig. 5: The spectra of TM nanoparticles, CS, SA, and TM

The FTIR spectra of TM nanoparticles in fig. 5 indicate the interaction among nanoparticles components. CS indicates a broad band appearing at 3354 cm^{-1}due the stretching vibrations of O-H/N-H. The peak at 2873 $cm^{-1}$is due C-H stretching vibrations. The band for C≡C stretching vibrations appears at 2113.39 cm^{-1}. The weak peak at 1645 $cm^{-1}$is due to C=N stretching vibrations. The peak at 1419.57 $cm^{-1}$is due to O-H bending vibrations. The C-O stretching vibrations appears at wavenumber 1149.91 cm^{-1}, 1061.63 cm^{-1}, and 1025.46 cm^{-1}, respectively. The peak at 894.14 cm^{-1} is due to C-H bending vibrations. Meanwhile, SA indicates a broadband appearing at 3357 cm^{-1}due to O-H stretching vibrations. The band for C≡C stretching vibrations appears at 2099.39 cm^{-1}. The peak at 1597.67 cm^{-1} is due to C=C stretching vibrations. The peak at 1409.45 cm^{-1}appears due to O-H bending vibrations. The C-O stretching vibrations appears at wavenumber 1295.48 cm^{-1} and 1086.80 cm^{-1}, respectively. The peak at 882.52 cm^{-1} is due to C-H bending vibrations.

TM indicates a band appearing at wavenumber 3283.15 cm^{-1} due to O-H stretching vibrations. The C-H stretching vibrations appears at wavenumber 3039.76 cm^{-1}, 2964.64 cm^{-1}, 2890.35 cm^{-1}, and 2852.60 cm^{-1}, respectively. Meanwhile, the C-H bending vibrations appears at wavenumber 1980.62 cm^{-1}. The peaks at wavenumber 1702.20 $cm^{-1}$is due to C=O stretching vibrations. The C=N stretching vibrations appears at wavenumber 1618.42 cm^{-1}. There are peaks at 1489.02 and 1448.64 cm^{-1}due to the N-H bending and O-H bending vibrations. The peak at wavenumber 1380.43 $cm^{-1}$is due S-N vibrations. There are peaks indicate the C-O stretching vibrations at wavenumber 1292.88 cm^{-1}, 1262.02 cm^{-1}, 1227.27 cm^{-1}, 1197.37 cm^{-1}, 1054.22 cm^{-1}, respectively. The C=C bending vibrations appears at wavenumber 988.17 cm^{-1}, 954.49 cm^{-1}, 890.02 cm^{-1}, 861.08 cm^{-1}, and 806.50 cm^{-1}, respectively.

After loading TM in the nanoparticles, there is broadband at wavenumber 3354.92 cm^{-1} due to O-H stretching vibrations. The band for C≡C stretching vibrations appears at wavenumber 2106.60 cm^{-1}. Both of these peaks are similar to the peak of CS and SA. There is a sharp peak at wavenumber 1603.44 cm^{-1} due to C=N stretching vibrations. The peaks at 1416.91 cm^{-1} due to O-H bending vibrations. The peaks indicate the C-O stretching vibrations at wavenumber 1076.31 cm^{-1} and 1026.10 cm^{-1}, respectively. These peaks are also simillar to the peak of CS and SA. There are peaks at wavenumber 888.67 cm^{-1} and 817.51 cm^{-1} due to C=C bending vibrations. These peaks are simillar to peak of TM. These results confirmed with the characterization of nanoparticles component, so that indicated TM loaded in the nanoparticles system.

Ionic interaction involved an ionic cross-linking between cations on the backbone of CS and anion of SA [25]. $CaCl_2$ was used as stabilizer, which contributed to the formation of the particle core. Although SA can be complex with CS alone and can form nanoparticles through formation of a simple polyelectrolyte complex, the formation of a pre-gel phase between Ca^{2+}ions and SA allows the formation of nanoparticles with increased compact structure [22]. Ionic interaction of TM, CS, SA, and $CaCl_2$ was showed in fig. 6.

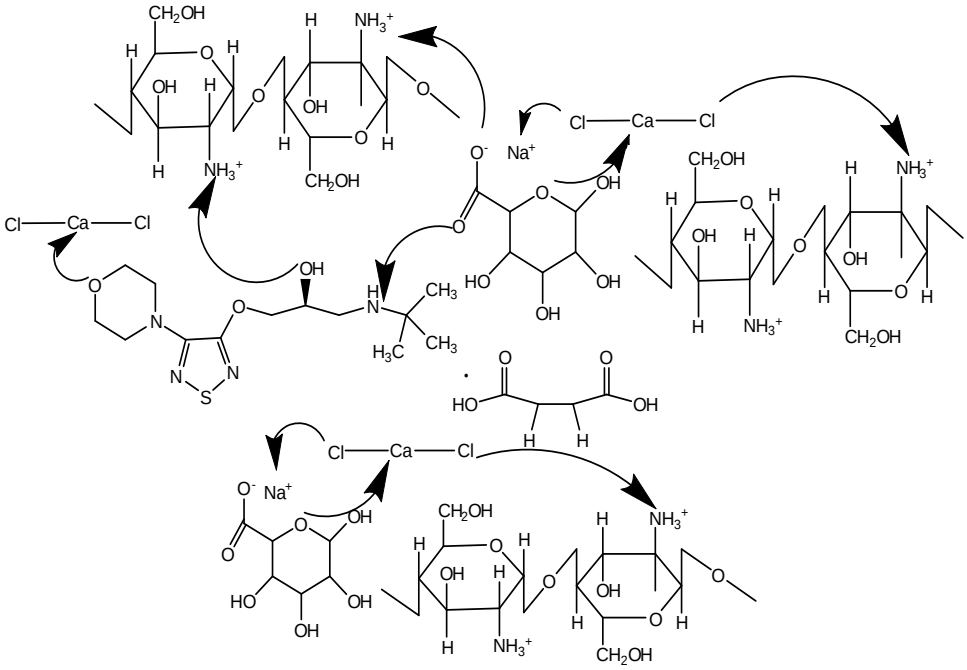

Fig. 6: Ionic interaction of TM, CS, SA, and $CaCl_2$

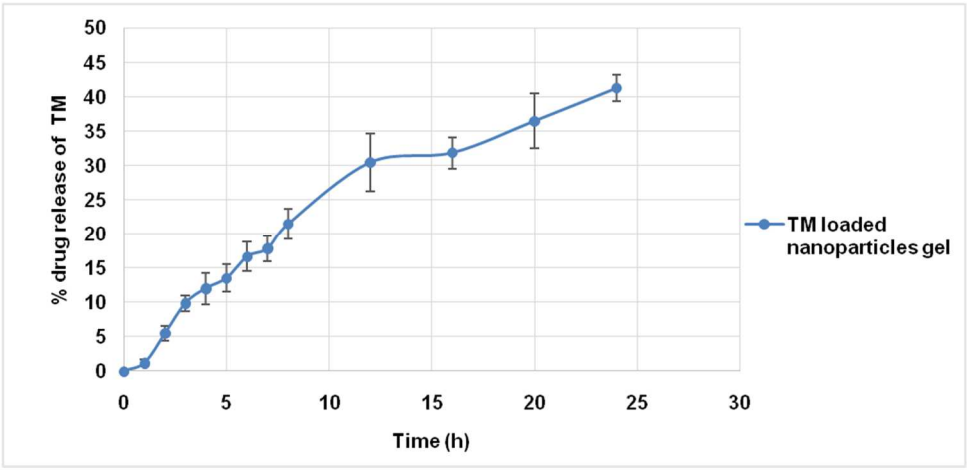

Fig. 7: The release profile of TM-loaded nanoparticles gel in PBS (data is presented in mean±SD (n=3))

***In vitro* release study**

The release profile of TM from nanoparticles gel in PBS was showed in fig. 7.

Fig. 7 showed the controlled release patern of TM from nanoparticles gel and it showed % drug release 41.21±1.94 % in 24 h. The *in vitro* release profile exhibited a controlled release phase lasting for long period. The controlled release phase may be attributed to the swelling or degradation of the polymer, which leads to the formation of pores within the polymeric matrix [26]. This result was also in accordance with the previously study that reported drug release was sustained for a long period which may be due to the hydration capability of CS which on coming in contact with dissolution medium result to the formation of gelatinous mass that act as a retardant material for the drug to get diffused out [27].

The data obtained from *in vitro* release study of TM from CS/SA nanoparticles gel was further analysed with different kinetic models (zero orde, first orde, Higuchi, Korsmeyer-Peppas, and Hixson-Crowell). Hence, the Korsmeyer-Peppas model was found to be the best fit for drug release kinetics. Korsmeyer-Peppas is a mathematical model that describes drug release from polymeric system [28]. The finding was also in accordance with the previously study [29, 30]. These studies reported that Korsmeyer-Peppas is the best fit of drug release from nanoparticle polymeric system. Mathematical Model in TM Release Kinetics was showed in table 2.

Table 2: Mathematical model in TM release kinetics

Mathematical model in drug release kinetics	Parameter	Number		
		1	**2**	**3**
Zero order	K_0	1.916	2.176	1.878
	R^2 adj	0.9138	0.8569	0.9171
	AIC	69.3402	78.1404	67.8008
	MSC	2.1397	1.6045	2.1689
First Order	K_1	0.024	0.028	0.023
	R^2 adj	0.9649	0.9387	0.9639
	AIC	57.6507	67.1089	56.9825
	MSC	3.0389	2.4530	3.0011
Higuchi	K_H	7.327	8.427	7.193
	R^2 adj	0.9116	0.9341	0.9241
	AIC	69.6712	68.0689	66.6619
	MSC	2.1142	2.3792	2.2565
Korsmeyer-Peppas	K_{K-P}	4.108	5.650	4.133
	R^2 adj	0.9741	0.9677	0.9826
	AIC	54.5676	59.6611	48.3646
	MSC	3.2761	3.0259	3.6640
	N	0.727	0.658	0.718
Hixson-Crowel	K_{H-C}	0.007	0.009	0.007
	R^2 adj	0.9516	0.9169	0.9515
	AIC	61.8455	71.0739	60.8425
	MSC	2.7162	2.1480	2.7042

*Constant release of drug (K). Coefficient of Determination (R^2 adjusted) expressed as the relationship between the data obtained from TM observed release study and the predicted model. Akaike Information Criterion expressed as the parameters used to select the appropriate model by comparing the values of the models (the selection of the appropriate model is based on the smallest for AIC value). Model Selection Factor (MSC) expressed as compatibility between the model and data (the selection of the appropriate model is based on the highest for MSC value). Data from each parameter is presented in replication (n=3).

CONCLUSION

We have prepared successfully TM-loaded nanoparticles gel by ionic gelation using biopolymer CS and SA. The best formula was prepared with concentration of CS, SA, and $CaCl_2$ of 0.01 % w/v, 0.1 % w/v, and 0.25 % w/v, respectively. The particle size, polydispersity index, entrapment efficiency, and Zeta potential were found to be 200.47±4.20 nm, 0.27±0.0154, 35.23±4.55 %, and-5.68±1.80 mV, respectively. The result of FTIR spectra indicated TM loaded in the nanoparticles system. *In vitro* release profile of TM-loaded nanoparticles gel showed controlled release and Korsmeyer-Peppas model was found to be the best fit for drug release kinetics. Finally, we concluded that TM-loaded CS/SA nanoparticles gel can be considered as a promising candidate for controlled TM delivery of IH treatment.

ACKNOWLEDGMENT

Author thanks to The Ministry of Research, Technology, and Higher Education of the Republic of Indonesia for its grant so that this research can be done.

AUTHORS CONTRIBUTIONS

RA compiled data dan prepared manuscript. LN, RM and RD designed research, analysed data, and made critical thinking on the manuscript.

CONFLICT OF INTERESTS

The author declares that there is no conflict of interest.

REFERENCES

1. Ariwibowo L, Budiyanto A, Danarti R. Efikasi terapi topikal corticosteroid ultra potent, solusio, dan gel timolol maleat 0,5% terhadap hemangioma infantil superfisial. Sari Pediatri 2016;17:428-34.
2. Pope E, Krafchik BR, Macarthur C, Stempak D, Stephens D, Weinstein M. Oral versus high dose pulse corticosteroids for problematic infantile hemangiomas: a randomized, controlled trial. Pediatrics 2007;119:1239-47.
3. Callahan AB, Yoon MK. Infantile hemangiomas: a review. Saudi J Ophthalmol 2012;26:283–91.
4. Weissenstein A, Straeter A, Villalon G, Bittmann S. Topical timolol for small infantile hemangioma: a new therapy option. Turk J Pediat 2012;54:156-8.
5. Danarti R, Ariwibowo L, Radiono S, Budiyanto A. Topical timolol maleate 0.5% for infantile hemangioma: its effectiveness compared to ultrapotent topical corticosteroids-a single-center experience of 278 cases. Dermatology 2016; 232:566–71.
6. McMahon P, Oza V, Frieden IJ. Topical timolol for infantile hemangiomas: putting a note of caution in "cautiously optimistic": commentary. Pediatric Dermatol 2012;29:127–30.
7. Mohanraj VJ, Chen Y. Nanoparticles-a review. Trop J Pharm Res 2006;5:561-73.
8. Sarangi MK, Padhi S. Solid lipid nanoparticles–a review. J Crit Rev 2016;3:5-12.
9. Kasar PD, Kale KS, Phadtare DG. Nanoplex: a review of the nanotechnology approach for solubility and dissolution rate enhancement. Int J Curr Pharm Res 2018;10:6-10.
10. Lertsutthiwong P, Rojsitthisak P. Chitosan-alginate nanocapsules for encapsulation of turmeric oil. Pharmazie 2011;66:911–5.
11. Martien R, Irianto IDK, Farida V, Sari P. Perkembangan teknologi nanopartikel sebagai sistem penghantaran obat. Majalah Farmaseutik 2012;8:134-44.
12. Li P, Dai YN, Zhang JP, Wang AQ, Wei Q. Chitosan-alginate nanoparticles as a novel drug delivery system for nifedipine. Int J Biomed Sci 2008;4:221-8.
13. Muhtadi WK, Novitasari L, Martien R, Danarti R. Factorial design as the method in the optimization of timolol maleate-loaded nanoparticle prepared by ionic gelation technique. Int J Appl Pharm 2019;11:66-70.
14. Ilka R, Mohseni M, Kianirad M, Naseripour M, Ashtari K, Mehravi B. Nanogel-based natural polymers as smart carriers for the controlled delivery of timolol maleate through the cornea for glaucoma. Int J Biol Macromol 2018;109:955–62.
15. Daemi H, Barikani M. Synthesis and characterization of calcium alginate nanoparticles, sodium homopolymannuronate salt and its calcium nanoparticles. Sci Iranica 2012;19:2023–8.
16. Manish K, Kulkarni GT. Development and process optimization of variables for the preparation of novel polymeric nanoparticles containing azelastine hydrochloride. J Pharm Res 2012;5:4884-7.
17. Raditya I, Effiniora A, Mahdi J. Preparasi nanogel verapamil hidroklorida menggunakan metode gelasi ionik antara kitosan-natrium tripolifosfat sebagai sediaan antihipertesi. Jurnal Farmasi Indonesia 2013;6:201-10.

18. Pham DT, Saelim S, Tiyaboonchai W. Design of experiments model for the optimization of silk fibroin based nanoparticles. Int J Appl Pharm 2018;10:195-201.
19. Galih P, Ronny M, Retno M. Chitosan nanoparticle as a delivery system for polyphenols from meniran extract (Phyllanthus niruri L.): formulation, optimization, and immunomodulatory activity. Int J Appl Pharm 2019;11:50-8.
20. Sumathi R, Tamizharasi S, Sivakumar T. Formulation and evaluation of polymeric nanosuspension of naringenin. Int J Appl Pharm 2017;9:60-70.
21. Manimekalai P, Dhanalakshmi R, Manavalan R. Preparation and characterization of ceftriaxone sodium encapsulated chitosan nanoparticles. Int J Appl Pharm 2017;9:10-5.
22. Morsi N, Ghorab D, Refai H, Teba H. Preparation and evaluation of alginate/chitosan nanodispersions for ocular delivery. Int J Pharm Pharm Sci 2015;7:234-40.
23. Huang J, Peng T, Li Y, Zhan Z, Zeng Y, Huang Y, *et al.* Ocular cubosome drug delivery system for timolol maleate: preparation, characterization, cytotoxicity, ex vivo, and *in vivo* evaluation. AAPS PharmSciTech 2017;18:2919-26.
24. Yap KYL, Chan SY, Lim CS. Infrared-based protocol for the identification and categorization of ginseng and its products. Food Res Int 2007;40:643–52.
25. Hussain Z, Sahudin S. Preparation, characterisation and colloidal stability of chitosan-tripolyphosphate nanoparticles: optimization of formulation and process parameters. Int J Pharm Pharm Sci 2016;8:297-308.
26. Chaiyasan W, Srinivas SP, Tiyaboonchai W. Development and characterization of topical ophthalmic formulations containing lutein-loaded mucoadhesive nanoparticles. Int J Pharm Pharm Sci 2016;8:261-6.
27. Sarkar T, Ahmed AB. Development and *in vitro* characterization of chitosan loaded paclitaxel nanoparticle. Asian J Pharm Clin Res 2016;9 Suppl 3:145-8.
28. Korsmeyer RW, Gurny R, Doelker E, Buri P, Peppas NA. Mechanisms of solute release from porous hydrophilic polymers. Int J Pharm 1983;15:25–35.
29. Mukhopadhyay P, Chakrabortya S, Bhattacharyab S, Mishrab R, Kundua PP. pH-sensitive chitosan/alginate core-shell nanoparticles for efficient and safe oral insulin delivery. Int J Bio Macromol 2015;72:640–8.
30. Nagarwal RC, Kumar R, Pandit JK. Chitosan coated sodium alginate–chitosan nanoparticles loaded with 5-FU for ocular delivery: *in vitro* characterization and *in vivo* study in the rabbit eye. Eur J Pharm Sci 2012;47:678–85.